OPTOELECTRONICS AND ADVANCED MATERIALS – RAPID COMMUNICATIONS Vol. 16, No. 9-10, September-October 2022, p. 453 - 457

Characterization of CdSe thin film fabricated by electrodeposition

S. ILDAN OZMEN[1,*], H. METIN GUBUR[2]
[1]*Advanced Technology Education Research and Application Center, Mersin University, Mersin, Turkey*
[2]*Department of Physics, Mersin University, Mersin, Turkey*

CdSe semiconductors that have a direct band gap and high absorption coefficient are quite suitable materials for photovoltaic devices. The production of semiconductors with a cheap and simple method is very important in terms of cost reduction. This paper consists fabrication of CdSe thin film with electrodeposition which cheap and simple method. The electrodeposition was carried out in an aqueous solution consisting low concentration of $CdCl_2$ and TeO_2 at room temperature on indium tin oxide coated glass substrate (ITO) with a 1 mA/cm^2 current density. The characterization of CdSe semiconductors thin film was made by UV-visible spectrophotometer, XRD (X-ray Diffraction), Raman spectroscopy, SEM (Scanning Electron Microscopy), EDX (Energy Dispersive X-ray Spectroscopy) and Hall-effect measurement. The CdSe thin film was found to have a hexagonal structure and a 1.71 eV energy band gap. The CdSe film has a chemical composition of 55 % Cd and 45 % Se. The carrier concentration of n-type CdSe film was measured as 8.80 x 10^{17} cm^{-3}.

(Received April 7, 2022; accepted October 5, 2022)

Keywords: Electrodeposition, CdSe thin film, Structural and optical characterization

1. Introduction

Due to their wide range of properties, metal chalcogenide materials are used in applications such as electronics, optics, magnetics, solar energy conversion, catalysis, batteries and fuel cells [1]. CdSe is a metal chalcogenide material, which has a direct energy band gap and high optical absorption coefficient, belonging to the II-VI group [2, 3]. CdSe thin films have been investigated in optoelectronic devices such as solar cells, photoconductors, thin film transistors, and gamma ray detectors because of direct band gap energy of 1.74 eV and high light sensitivity in the visible region [4–7].

CdSe has cubic, hexagonal structures or mixtures of two structures and it displays n-type or p-type semiconductor properties [2, 8]. The fabrication technique affects the morphologic, optical, structural, and electrical properties of the CdSe thin films. Various fabrication techniques have been used to obtain CdSe thin films such as chemical bath deposition [9, 10], physical vapor deposition [11, 12], chemical vapor deposition [13], thermal evaporation [14], electrodeposition [15, 16], etc. Electrodeposition is essential in these techniques because it has a simple application and is inexpensive. Also, it is a technique that the film's morphological, structural, and electrical properties can be easily controlled by concentration, pH, temperature, current and potential [4, 17, 18].

Many researchers have used the electrodeposition technique to obtain CdSe films. They have generally electrodeposited the CdSe thin films at constant potential as potentiostatic [5, 6, 15, 19, 20]. Also, there are some studies about the CdSe thin films that were achieved at various temperatures using the constant potential [3, 4, 6, 8]. Arif V. Shaikh et al. have used a constant cathodic current density for electrodeposition of CdSe thin film from a solution containing EDTA with a pH of 10 [21]. In this study, CdSe thin film was obtained by electrodeposition technique in acidic aqueous solution at room temperature at constant current density. We have seen that hexagonal CdSe thin films with n-type conductivity and a 1.71 eV energy band gap may be easily produced by electrodeposition without the use of heat.

2. Experimental details

CdSe thin film was electrodeposited on ITO coated glass (surface resistivity 8-12 Ω/sq) in aqueous solution consist of 0.1 M $CdCI_2$ (Acros, 99%) and 0.1 mM SeO_2 (Sigma, 98%). The pH of the solution was adjusted to ~2 with HCI (Merck, 37%). For the electrochemical deposition set up platin sheet and Ag/AgCI (3.5M KCI) were used respectively as counter and reference electrodes. CHI 660D Electrochemical Workstation was used for electrodeposition. The CdSe thin film was electrodeposited at room temperature cathodically with a 1 mA / cm^2 current density during 60 minutes. It was seen that the deposition took place at about -0.95 V from the potential – time diagram. The substrate was cleaned with ethanol, propanol, acetone, ultrapure water and dried with an air dryer before and after the deposition process.

Optical transmittance spectrum of the CdSe thin film was measured by the UV-visible spectrophotometer (Shimadzu UV-1700) that wavelength range of 190-1100 nm and the optical band gap of the film was obtained from the transmittance spectrum. XRD pattern was recorded by Rigaku Smart Lab X-ray diffractometer using CuKα radiation (λ = 1.54 Å) of 20°≤ 2θ°≤ 60°, and 0.02° steps. Raman measurement was done using a Renishaw inVia Qontor Raman microscope at 785 nm wavelength. The SEM images of the film were obtained with a Zeiss-Supra 55 FE-SEM. The chemical composition of the CdSe film was investigated using Energy Dispersive X-ray Spectroscopy (EDX). The resistivity, carrier concentration, and mobility were determined in a Van der Pauw four-point probe configuration, using gold contacts with a magnetic induction of 0.54 T at room temperature.

3. Results and discussion

3.1. Optical properties

Optical properties of CdSe electrodeposited on ITO substrate has been investigated with UV-visible spectroscopy in the wavelength range from 300 nm to 1100 nm. The transmission versus wavelength spectrum of the CdSe thin film is displayed the inset in Fig. 1. The thickness of the film was calculated using the transmission interferences in this spectrum by the following equation:

$$d = \left[\frac{\lambda_1 \lambda_2}{2n(\lambda_2 - \lambda_1)}\right] \quad (1)$$

where d is the film thickness, n the refractive index, λ_1 and λ_2 are at the two adjacent maxima (or minima) [22]. CdSe thin film thickness is found ~147 nm.

The energy band gap of the semiconductor CdSe thin film was calculated by the correlation between the absorption coefficient and photon energy:

$$\alpha = A\left(h\nu - E_g\right)^n / h\nu \quad (2)$$

where A is a constant, α is absorption coefficient, $h\nu$ is the photon energy and n is also a constant and depends on the type of the transitions. n is 1/2 because CdSe has a direct optical transition. The Fig. 1 shows the α^2 versus photon energy (hv) diagram of the CdSe film. The Eg value of the CdSe thin film was obtained from the intercept on energy axis where $\alpha^2 = 0$ via extrapolating the linear portion of the graph. The optical band gap of the film was found at around 1.71 eV from the graph. This value is close to the 1.74 eV energy band gap of bulk CdSe [5, 23].

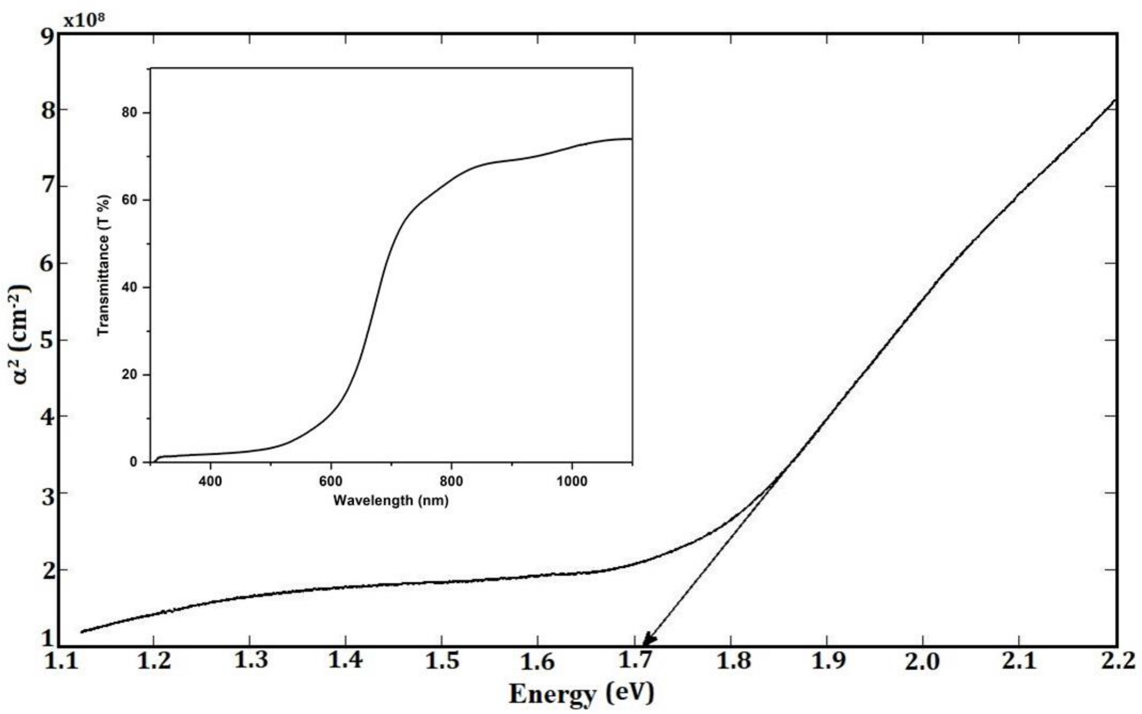

Fig. 1. The α^2 versus photon energy (hv) diagram of the CdSe film and inset transmittance versus wavelength graphic

3.2. Morphological properties

Surface morphology of the CdSe thin film electrodeposited on ITO substate was investigated by SEM. Fig. 2 shows the SEM images of the CdSe morphology at (a) 200.00 KX and (b) 50.00 KX magnifications. It is seen that the CdSe film is uniformly distributed on the ITO substrate from SEM images. Also, SEM images show that the CdSe film was coated smoothly and homogeneously on the ITO surface. The elemental composition of the CdSe was found that 55 % Cd, 45% Se from EDX analysis, as given in Fig. 3.

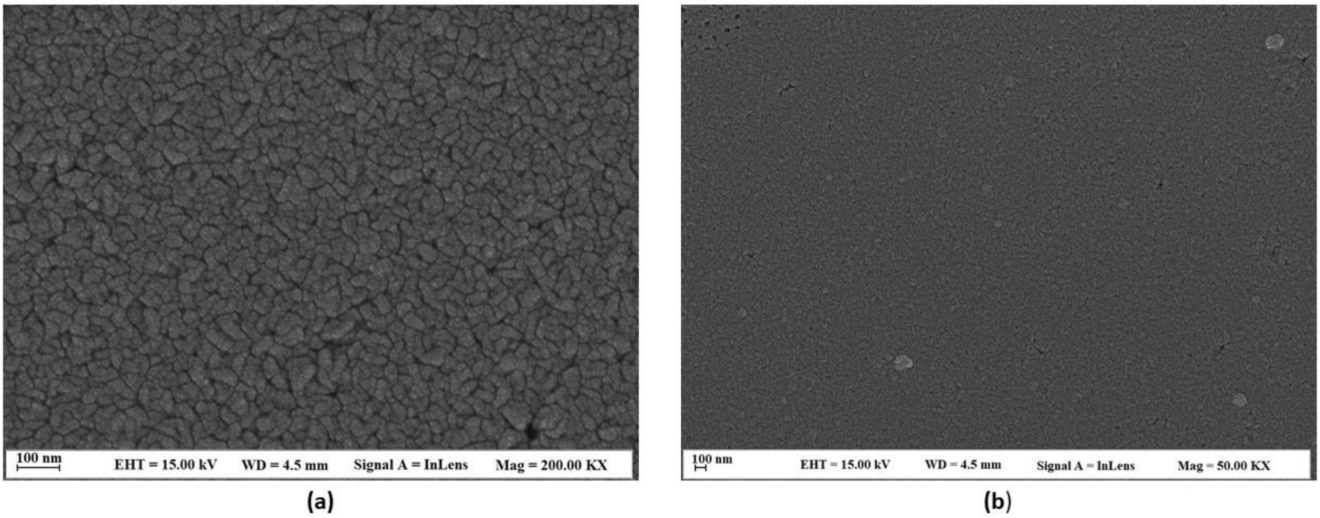

Fig. 2. The surface images of CdSe thin films at (a) 200.00 KX, and (b) 50.00 KX magnifications

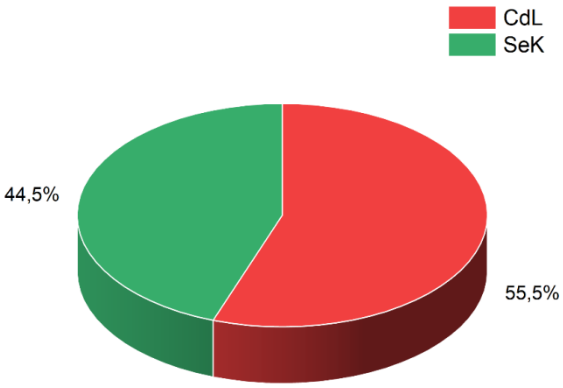

Fig. 3. The atomic percentage values of Cd and Se elements in the CdSe thin film (color online)

3.3. Structural properties

Fig. 4 shows XRD pattern of the electrodeposited CdSe thin film on ITO substrate. It was determined that the (100), (002), (101), (102), (110) and (112) diffraction peaks seen in the CdSe film matched with the JCPDS reference card numbered 01-075-5679 and the crystal structure was hexagonal. It has been reported in previous studies that CdSe thin films obtained by electrodeposition have cubic [2, 4, 6], hexagonal [5,24], and polycrystalline [19, 21, 25] structures.

The average crystallite size was calculated using Scherrer equation,

$$D_{hkl} = \frac{K\lambda}{\beta \cos\theta} \tag{3}$$

Here, λ is the wavelength of the X-ray used, θ is the Bragg reflection angle, β is the half-maximum width (FWHM) in radians, and K is a constant of 0.9 in the calculations.

The dislocation density was calculated using the crystallite size data with Equation (4):

$$\delta = {}^{1}\!/_{D_{hkl}^{2}} \tag{4}$$

The number of crystals per unit surface was calculated using Equation (5):

$$N = {}^{d}\!/_{D_{hkl}^{3}} \tag{5}$$

Here, d is the film's thickness. Strain was calculated using Equation (6):

$$\varepsilon = \beta \cos\theta / 4 \tag{6}$$

All calculated parameters of CdSe thin film according to selected diffraction peaks are given in Table 1.

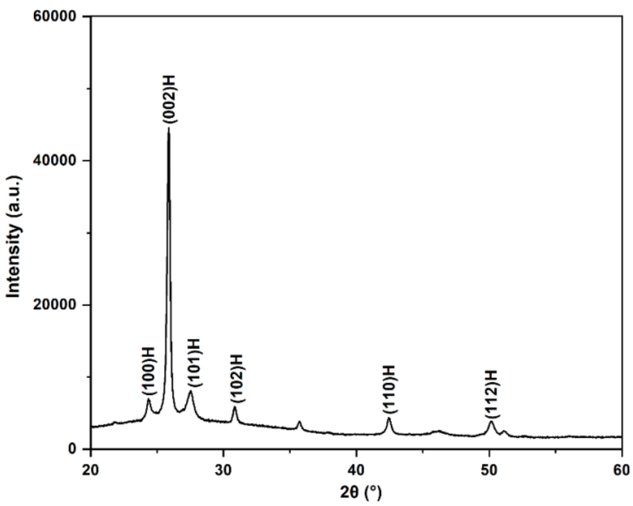

Fig. 4. The XRD pattern of CdSe thin film

Table 1. The FWHM, crystallite size, dislocation density, number of the crystallites/unit area, and strain of the CdSe film

(hkl)	**(002)**
Crystal structure	Hexagonal
FWHM (deg)	0.21
D (nm)	38.80
δ (10^{14} line/m^2)	6.64
N (10^{22} m^{-2})	5.89
ε (10^{-4})	8.93

Raman spectroscopy is an important method to further investigation of structural analysis. The Raman spectrum of the hexagonal CdSe thin film is displayed in Fig. 5. There are three active modes seen in Raman shift spectra at 175 cm^{-1}, 202 cm^{-1}, and 402 cm^{-1}. The observed peak at 202 cm^{-1} is related to the longitudinal optical (LO) phonon mode of the nanocrystalline CdSe [16, 26–29]. The weak peak at 402 cm^{-1} corresponds to the second longitudinal optical (2LO) phonon mode of CdSe nanocrystals [16,28–30]. The Raman peak is observed at 175 cm^{-1} is assigned to the transverse optical (TO) mode [13, 16].

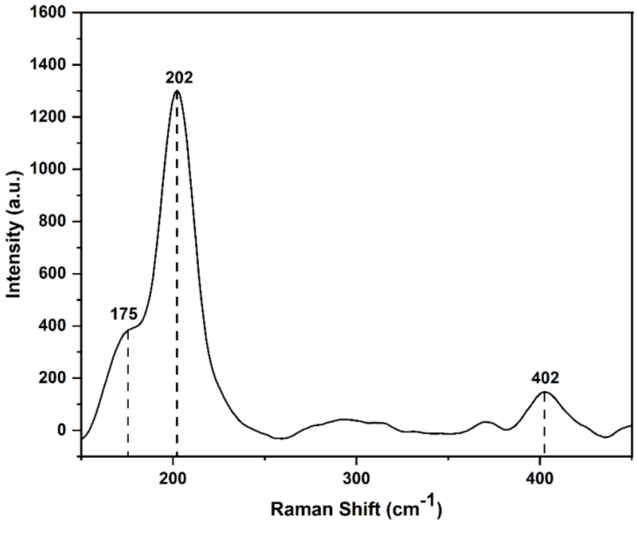

Fig. 5. The Raman spectra of CdSe thin film

3.4. Electrical properties

The electrical properties such as carrier type, carrier density (cm^{-3}), mobility (cm^2/Vs), and resistivity (Ω - cm) of the CdSe thin film were determined at room temperature by the Hall effect measurement. The carrier type of the films was found by sign of Hall coefficient. CdSe thin film's carrier type was identified as n-type because Hall coefficient was negative. The carrier density, mobility, and resistivity of the CdSe film were respectively 8.80 × 10^{17} cm^{-3}, 1.06 cm^2/Vs, and 6.69 Ω - cm. When these results are compared with the studies in which the CdSe thin films are obtained by electrodeposition, it is seen that the resistance is lower [5, 24], and the carrier concentration is higher [15, 25].

4. Conclusions

The CdSe thin film was simply electrodeposited on ITO substrate cathodically in an aqueous solution at room temperature. It is significant using a simple and cheap method to the fabrication of the films for cost reduction and ease of application. The electrodeposited CdSe film was coated on ITO substrate homogenously as nanosized particles. Energy band gap and absorption coefficient of the film was determined 1.71 eV and 10^5 cm^{-1}, respectively. The structure of the CdSe film was found hexagonal and the characteristic Raman shifts of the nanocrystal CdSe were seen from the Raman analysis. The carrier type was identified n-type by Hall measurement.

Acknowledgments

This study was supported by the Research Fund of Mersin University in Turkey with Project Numbers: 2017-2-TP3-2593.

References

[1] M. Bouroushian, Electrochemistry of metal chalcogenides, Springer Berlin Heidelberg, 2010.
[2] H. Bayramoglu, A. Peksoz, Mater. Sci. Semicond. Process. **90**, 13 (2019).
[3] M. Bouroushian, C. Kollia, Z. Loizos, N. Spyrellis, G. Maurin, Appl. Surf. Sci. **102**(96), 112 (1996).
[4] A. Y. Shenouda, E. S. M. El Sayed, Ain Shams Eng. J. **6**(1), 341 (2015).
[5] R. Mariappan, V. Ponnuswamy, S. M. Mohan, P. Suresh, R. Suresh, Mater. Sci. Semicond. Process. **15**(2), 174 (2012).
[6] M. Bouroushian, Z. Loïzos, N. Spyrellis, G. Maurin, Thin Solid Films **229**(1), 101 (1993).
[7] S. Mahato, N. Shakti, A. K. Kar, Mater. Sci. Semicond. Process. **39**, 742 (2015).
[8] S. Hamilakis, N. Gallias, C. Mitzithra, K. Kordatos, C. Kollia, Z. Loizos, Mater. Lett. **143**, 63 (2015).
[9] H. Gubur Metin, F. Septekin, S. Alpdogan, J. Korean Phys. Soc. **67**(7), 1222 (2015).
[10] F. Oksuzoglu, H. Metin Gubur, A. K. Havare, S. Ildan Ozmen, M. Unal, C. Tozlu, J. Photonics Energy **10**(2), 1 (2020).
[11] M. Morales-Luna, M. A. Arvizu, M. Pérez-González, S. A. Tomás, J. Phys. Chem. C **123**, 17083 (2019).
[12] S. Devadason, M. R. Muhamad, Phys. B Condens. Matter. **393**, 125 (2007).
[13] R. Venugopal, P. I. Lin, C. C. Liu, Y. T. Chen, J. Am. Chem. Soc. **127**(32), 11262 (2005).

[14] M. S. Al-Kotb, J. Zamel Al-Waheidi, M. F. Kotkata, Superlattices Microstruct. **55**, 131 (2013).
[15] V. S. Raut, C. D. Lokhande, V. V. Killedar, J. Electroanal. Chem. **788**, 137 (2017).
[16] R. Bai, S. Chaudhary, D. K. Pandya, 3rd Int. Conf. Condens. Matter Appl. Phys. **2220**, 020044 (2020).
[17] A. Mayabadi, K. Mirabbaszadeh, A. Pawbake, S. Rondiya, A. Rokade, R. Waykar, R. Kulkarni, H. Pathan, S. Jadkar, J. Mater. Sci. Mater. Electron. **28**, 18745 (2017).
[18] H. Luo, L. G. Ma, W. M. Xie, Z. L. Wei, K. G. Gao, F. M. Zhang, X. S. Wu, Appl. Phys. A Mater. Sci. Process. **122**(444), 1 (2016).
[19] S. Alam, M. A. K. Pathan, K. A. M. H. Siddiquee, A. B. M. O. Islam, M. A. Gafur, D. K. Saha, M. Mori, T. Tambo, Optik **124**, 2165 (2013).
[20] K. Yu-Zhang, D. Z. Guo, J. Mallet, M. Molinari, A. Loualiche, M. Troyon, J. Nanosci. Nanotechnol. **8**(4), 2022 (2008).
[21] A. V. Shaikh, R. S. Mane, O. S. Joo, B. N. Pawar, J. K. Lee, S. H. Han, J. Phys. Chem. Solids **72**(10), 1122 (2011).
[22] J. Acque. I. Pankove, Optical Processes in Semiconductors. New York: Dover Publications, Inc., 1971.
[23] F. Majid, A. Malik, S. Ata, Z. Hussain, I. Bibi, M. Iqbal, M. Rafay, H. Rizvi, Z. Phys. Chem. **233**(9), 1 (2018).
[24] H. Soonmin, C. U. Vyas, P. Pataniya, K. D. Patel, S. Mahato, Mediterr. J. Chem. **7**(2), 115 (2018).
[25] V. Swaminathan, V. Subramanian, K. R. Murali, Thin Solid Films **359**(1), 113 (2000).
[26] A. M. Kelley, Q. Dai, Z. J. Jiang, J. A. Baker, D. F. Kelley, Chem. Phys. **422**, 272 (2013).
[27] P. V. Teredesai, F. L. Deepak, A. Govindaraj, A. K. Sood, C. N. R. Rao, J. Nanosci. Nanotechnol. **2**(5), 495 (2002).
[28] G. X. Wang, M. S. Park, H. K. Liu, D. Wexler, J. Chen, Appl. Phys. Lett. **88**(19), 193115 (2006).
[29] V. V. Antipov, S. A. Kukushkin, A. V. Osipov, V. P. Rubets, Phys. Solid State **60**(3), 504 (2018).
[30] D. Nath, R. Das, Appl. Surf. Sci. **509**, 144708 (2020).

*Corresponding author: sevdaildan@mersin.edu.tr